Received: 18 April 2022 | Revised: 10 July 2022 | Accepted: 16 July 2022

DOI: 10.1002/hipo.23459

RESEARCH ARTICLE

WILEY

Prefrontal and hippocampal theta rhythm show anxiolytic-like changes during periaqueductal-elicited "panic" in rats

Carlos Silva | Calvin K. Young | Neil McNaughton

Department of Psychology and Brain Health Research Centre, University of Otago, Dunedin, New Zealand

Correspondence
Neil McNaughton, Department of Psychology, University of Otago, PO Box 56, Dunedin 9054, New Zealand.
Email: neil.mcnaughton@otago.ac.nz

Funding information
Coordenação de Aperfeiçoamento de Pessoal de Nível Superior, Grant/Award Number: BEX: 13064134; Ministério da Educação

Abstract

Anxiety and panic are both elicited by threat and co-occur clinically. But, at the neural level, anxiety appears to inhibit the generation of panic; and vice versa. Anxiety and panic are thought to engage more anterior (a) and mid-posterior (m) parts of the periaqueductal gray (PAG), respectively. Anxiety also engages the hippocampus and medial prefrontal cortex. Here, we tested if mPAG but not aPAG stimulation would suppress prefrontal and hippocampal theta rhythm as do anxiolytic drugs. Twelve male rats with implanted electrodes were stimulated alternately (30 s interval) in the left PAG or right reticular formation (reticularis pontis oralis [RPO]—as a positive control) with recording in the left prelimbic cortex and left and right hippocampus. PAG stimulation was set to produce freezing and RPO to produce 7–8 Hz theta rhythm before tests lasting 10 min on each of 5 days. mPAG stimulation decreased, and aPAG increased, theta power at all sites during elicited freezing. mPAG, but not aPAG, stimulation decreased prefrontal theta frequency. Stimulation did not substantially change circuit dynamics (pairwise phase consistency and partial directed coherence). Together with previous reports, our data suggest that panic- and anxiety-control systems are mutually inhibitory, and neural separation of anxiety and panic extends down to the aPAG and mPAG, respectively. Our findings are consistent with recent proposals that fear and anxiety are controlled by parallel neural hierarchies extending from PAG to the prefrontal cortex.

KEYWORDS
hippocampus, panic, periaqueductal gray, prefrontal cortex, theta

1 | INTRODUCTION

Both in normal life and psychopathology, there are complex interactions between different types of defensive responses. Knowing how survival circuits (LeDoux, 2012; Mobbs & LeDoux, 2018) interact and react dynamically with areas such as the more recently evolved prefrontal cortex (LeDoux, 2021) during these states is crucial if we are to understand them.

There is a reason to see the archicortex of the hippocampus as a key mediator between these higher and lower levels. Papez (1937) saw the hippocampus is a key node for processing emotion (see also Vann & Nelson, 2015; McNaughton & Vann, 2022). Then, the hippocampus was seen as more dedicated to memory. But there is a evidence that hippocampal damage alters emotion (Davidson et al., 2005, 2009; Tracy et al., 2001) and is a key control center for stress and hormones (Lathe, 2001, 2004). The ventral hippocampus has been most clearly linked to

anxiety (Bannerman et al., 2004); but anxiolytics impair learning in the Morris water maze (McNaughton & Morris, 1987, 1992) and reliably reduce hippocampal theta rhythmicity (McNaughton et al., 2007) on which spatial learning depends (McNaughton et al., 2006). Here, we investigate the interactions of basic mechanisms of fear and anxiety with hippocampal and prefrontal theta rhythmicity.

In rodents, the most basic expression of high levels of fear (e.g., generated by a proximal predator) involves panic in the form of true freezing (i.e., not sensitive to anxiolytics; Blanchard & Blanchard, 1990a) if escape is not available; and in the form of running if escape is available (Blanchard & Blanchard, 1990b). Controlled freezing and undirected running are elicited simply by stimulation of the periaqueductal gray (PAG; De Molina & Hunsperger, 1962), which contains fundamental control centers for aversive and defensive responses (Silva & McNaughton, 2019). If the states induced by activation of the PAG are reflective of panic, then understanding them should illuminate and broaden our understanding of general fear- and specific panic-generating systems in the brain[1] and of how to treat their disorders in the clinic.

Increasing dorsal PAG stimulation intensity evokes a hierarchy of behavioral and autonomic responses like that elicited by increasing predatory threat (Evans et al., 2018). Moderate stimulation elicits freezing while stronger intensities elicit undirected escape responses consisting of running and/or jumping, similar to animals close to predators (Sudre et al., 1993). Pharmacological studies with panicolytic drugs show that dorsal PAG stimulation-elicited *escape* behavior is a reliable proxy for fear and panic in animals (Jenck et al., 1995). However, there has been less attention to dorsal PAG-induced *freezing*.

In contrast, the most basic expression of high levels of anticipatory anxiety (e.g., generated by the smell or memory of a predator) is a form of anxiolytic-sensitive immobility—a defensive quiescence that can involve distinctive postures such as "stretch attend" (Blanchard & Blanchard, 1990a). Particularly in operant conditioning to aversive stimuli, anticipatory immobility is often called "freezing." But unlike panic-related freezing, this anticipatory "contextual" form of freezing (whether innate or conditioned) is responsive to anxiolytic drugs (Conti et al., 1990) and is a model for human anxiety-related disorders in general (Tovote et al., 2016) and generalized anxiety in particular (Luyten et al., 2011).

Fear and anxiety appear to be mutually antagonistic. Defensive quiescence requires inhibition of any co-activated tendency to escape; while escape requires inhibition of both freezing and defensive quiescence. Conditioned anxiety that generates defensive quiescence inhibits escape-like responses induced by PAG activation (Magierek et al., 2003). Conversely, in humans with panic disorder, anxiety reduction can release panic attacks (Cohen et al., 1985; Klein, 1993; Mellman & Uhde, 1989). Furthermore, in rodents and humans, anxiety enhances pain sensitivity while fear reduces it (Rhudy & Meagher, 2000); and anxiety and fear are affected in opposite directions by the 5-HT system (Deakin & Graeff, 1991).

Here, we investigate forebrain local field potential (LFP) activity during immobility elicited by PAG stimulation. We contrast PAG stimulation with reticular stimulation that elicits hippocampal (HPC) theta rhythm, which is a reliable model for testing anxiolytic drug efficacy (McNaughton et al., 2007). Although reticular stimulation does not elicit an emotional response, HPC theta appears to be a key mechanism controlling anxiety (Gray & McNaughton, 2000; McNaughton & Gray, 2000); so we expect that increases and decreases in HPC theta will reflect respective changes in anxiety systems in areas such as prefrontal cortex (LeDoux, 2015) that can become entrained to HPC theta during activities such as risk assessment (Adhikari et al., 2010; Gordon, 2011; Padilla-Coreano et al., 2019; Young & McNaughton, 2009).

We also test if the anterior PAG can generate distinct forebrain responses from more posterior PAG, as previously anticipated (Silva & McNaughton, 2019). Although stimulation of both parts of the PAG evokes immobility, anatomical, biochemical, and functional evidence suggests that these two PAG regions are not similar. Could the immobility elicited by different levels of the PAG be electrophysiologically different (reflecting defensive quiescence versus true freezing)? Our hypothesis of panic-anxiety mutual antagonism predicts that electrically stimulating the middle PAG freezing would *reduce* forebrain theta while anterior PAG freezing would *increase* forebrain theta.

2 | METHODS

2.1 | Animal housing and handling

The subjects were 15 male Sprague–Dawley rats obtained from the University of Otago Hercus-Taieri Resource Unit and weighed between 150 and 200 g on arrival. Two were removed from the study due to health complications, and a third because it had stimulating electrodes located outside of the regions of interest. Data below are reported for the remaining 12 rats, divided, after histology, into two groups with stimulating electrodes in the anterior ($N = 5$) or mid-posterior ($N = 7$) PAG, respectively. On arrival, rats were caged in pairs, and given ad libitum access to food and water in a temperature-controlled room (20–22°C), on a 12 h light–dark cycle with lights on at 6 a.m. All data were collected during the light period of the cycle. Rats had 10 days to acclimatize to the laboratory with daily handling, and were scheduled for surgery once body weight was >300 g. All experiments were conducted in accordance with the New Zealand Animal Welfare Legislation, approved by the University of Otago Animal Ethics Committee (approval numbers 29/12 and 10/16).

2.2 | Local field potential recording and stimulation electrodes

The animals used in the current experiments were intended for use in a separate drug experiment not reported here and therefore were

[1]Throughout this article, we distinguish anxiety and fear as detailed in Gray and McNaughton (2000; for updated neurology see figure 12 in Silva & McNaughton, 2019) and so include the specific reactions of "panic" (and their control by the PAG) within the more general reactions of "fear" (and their control by a hierarchy of structures running from the PAG at the lowest level to prefrontal cortex at the highest). This differs at key points from alternative uses of these words, for example, Perusini and Fanselow (2015).

TABLE 1 Coordinates for stereotaxic implantations

	A–P (reference)	M–L (mm)	D–V (skull) (mm)	Angle (°)	Nose bar
Left PrL	+2.76 mm (Bregma)	+0.60	−4.50	0	Flat skull
Left HPC	−3.8 mm (Bregma)	+2.50	−2.90	0	Flat skull
Right HPC	−3.8 mm (Bregma)	−2.50	−2.90	0	Flat skull
Right RPO	−7 mm (Bregma)	−1.60	−6.50	0	Flat skull
Left dPAG	+1.32 mm (Lambda)	+2.30	−4.50	16	Flat skull
NI	−2.8 mm (Lambda)	+0.62	−5.16	10	−12.5 mm

Abbreviations: A–P, anterior–posterior; dPAG, dorsal periaqueductal gray; D–V, dorsal–ventral; HPC, hippocampus; M–L, medial–lateral; PrL, prelimbic cortex; RPO, reticular pontis oralis.

implanted with one of two different types of recording electrode arrays targeting the left prelimbic cortex (PrL) and the left and right hippocampus. All animals had bipolar stimulating electrodes implanted in the region of the right reticularis pontis oralis (RPO) and left PAG and a guide cannula for intracerebral drug injections aimed at the midline nucleus incertus. All testing reported here was conducted during an initial saline injection session before any drug injections had been tested. Recordings were referenced to a common screw electrode behind lambda and, during post-processing, subtraction of an adjacent pair within an array (based on histology) delivered a local "bipolar" signal for analysis. The ground was a length of bare silver wire (0.005″ diameter, AM Systems), and was wrapped around the outside of the implant prior to suturing. Both RPO and PAG stimulating electrodes were 0.005″ bipolar twisted stainless-steel wires (AM-Systems) with a 0.5 mm tip separation.

One type of recording array was multipolar (up to 11 electrodes per array; each electrode made from 0.001″ diameter nichrome wires, California Fine Wire Company) connected to a 32-pin mini array socket (Ironwood). For the HPC arrays, eight recording tips were spaced 200 μm apart to cover the dorso-ventral axis. For PrL, 11 tips were spaced 500 μm apart to cover most of the medial wall of the prefrontal cortex. For further details see Banstola et al. (2021).

The other recording type was bipolar or tripolar and built from twisted, PFA-insulated stainless steel wires with a 0.005″ thickness (AM-Systems) with gold pins that were inserted into a McIntyre connector (McIntyre & Molino, 1972). For the HPC arrays, two twisted wires with a tip separation of 0.6 mm were aimed at the hippocampal fissure and stratum oriens of CA1. For PrL, three twisted wires with a tip separation of 1 mm were aimed to span the dorso-ventral extent of the PrL.

2.3 | Surgical methods

Thirty minutes prior to the beginning of surgery all animals received a prophylactic dose of antibiotic Amphoprim (30 mg/kg). The rats were given ketamine and medetomidine (75 mg/kg and 0.5 mg/kg, s.c.) as anesthetics for surgery and given additional injections of ketamine if necessary, as determined by toe pinch reflex. As soon as voluntary movement ceased, atropine (0.05 mg/kg, s.c.) was administered to aid breathing. For inhalation anesthesia, an isoflurane vaporizer (E-Z Anesthesia) was used. An oxygen–isoflurane mixture was delivered at a rate of 1.5 L/min. The percentage of isoflurane in the mixture was regulated between 2% and 3% depending on the animal's toe-pinch reflex and breathing rate. Buprenorphine (0.1 mg/kg, s.c.) was administered for additional pain control.

The animal's scalp was then shaved, sterilized, and infiltrated with a combined solution of Marcaine (0.4 ml/kg) and Lidocaine (0.2 ml/kg) subcutaneously. Tricin (Jurox, Australia) was applied to the animal's eyes, which were also covered with a wet cotton pad for protection. The animal's head was secured to the stereotaxic frame using non-traumatic ear bars. During surgery, all animals rested on a heated pad in order to maintain body temperature.

After placement of the rat in the stereotaxic frame, a single incision was made in the scalp, the skin was retracted and the skull exposed, where holes for the electrodes were drilled. The coordinates for implantation are shown in Table 1. These animals also had a cannula implanted at the nucleus incertus experiments reported here. The dorsal–ventral coordinates used for implanting the guide cannula (Plastic One) were calculated so the tip would be 1 mm dorsal to the nucleus incertus.

Seven stainless steel screws were fixed to the periphery of the skull in order to secure the electrodes and cannula. The reference electrode consisted of an eighth screw posterior and lateral to lambda. A bare silver wire tightly wrapped around outside the screws acted as earth. Dental cement held the connector in position.

For animals that received injectable anesthesia, Antisedan (atipamezole, 2.5 mg/kg s.c.) was administered to reverse the effects of the medetomidine to facilitate recovery. For animals that received gaseous anesthesia, the isoflurane–oxygen ratio was dropped to 0% and animals received pure oxygen for 10 min. In both cases, carprofen (5 mg/kg, s.c.) was given to relieve post-operative pain. During surgery, 2 ml of 0.9% physiological saline (up to 10 ml in total) was periodically administered s.c. to maintain hydration.

The animals were then individually housed in a clean cage with free access to food and water. The animal's well-being and recovery were monitored for 7 days according to the University of Otago Animal Welfare guidelines using a standard monitoring sheet. After approximately 10 days, rats were grouped back into their original pairs.

2.4 | Behavioral apparatus

All animals were tested in a modified operant chamber (width: 24.5 cm, height: 18.5 cm, and depth: 30 cm), with its levers, lights, and feeding mechanisms removed. All walls were transparent acrylic except one, which was aluminum; the floor was composed of

cylindrical metal bars with a tray underneath. This operant box was placed inside a second chamber, which apart from a small hole on the ceiling through which the recording cable ran, was fully sealed from external light and noise. Illumination inside the chamber was provided by a red light, and a fan provided air recirculation and background noise. A small video camera inside the larger chamber provided a live video feed for experimenter observation.

Prior to any data collection, the rats were individually placed inside the observation box and allowed to explore for 50 min for five consecutive days. Before each exposure, the walls and floor of the observation box were cleaned with a 10% ethanol solution and allowed to dry.

2.5 | Electrical stimulation response thresholds

Stimulating currents for the PAG and RPO electrodes were delivered by a custom-built, constant current isolated stimulator controlled by custom software programmed in Visual Basic 6. Stimulation was set at 100 Hz with monophasic pulses with a width of 0.1 ms. Trains for the RPO stimulation were set to 1 s duration, and PAG trains were set to 8 s maximum duration.

In order to determine the ideal currents necessary to drive the desired responses from the PAG and RPO, rats were tested for 2 days before data acquisition. They were individually placed in the observation chamber and given 30 min to habituate with the tethers before testing.

First, the current for appropriate RPO responses was established. When animals were immobile, an initial current of 10 μA was delivered in a 1-s train. High-intensity currents can provoke undesired motor reactions in free-moving animals, so during the delivery of the current, the animal's behavior and real-time LFPs were observed. We defined the ideal response as one where repeated stimulation elicited clear HPC theta during the stimulation train with no evoked motor response. If no induced theta or motor responses were observed, the stimulating current was increased in 5 μA steps until the highest current that caused no motor responses was reached.

Following the determination of RPO-stimulation values, the animals were tested for PAG-evoked responses. The goal for the PAG stimulation was to establish the minimum current intensity necessary to induce the emotional response of freezing. Stimulation trains were 8 s long, and the first current was set at 10 μA, with increases in 5 μA steps until the desired freezing behavior was evoked.

After repeated PAG stimulations at the freezing threshold, RPO stimulations were conducted again in order to verify that the desired hippocampal responses were still being elicited. In all cases, the currents established for the RPO-stimulation before PAG activations were still effective in inducing hippocampal theta rhythmicity when tested while not moving.

2.6 | Data acquisition and processing

Local field potentials were acquired by a Micro1401 (CED) at a sampling rate of 512 Hz. The signal was passed through Grass Model 15 amplifiers, and hardware gain was set at ×5000 for all acquired data. The signals acquired from the recording electrodes were referenced to the recording screw positioned at the posterior part of the rat's skull behind lambda in an electrically silent zone—but note that, for analysis, local bipolar re-referencing was used as described below. For data processing, the files were down-sampled to 256 Hz using the in-built cubic spline interpolation in Spike2 (CED), bandpassed at 2–30 Hz and exported to Matlab (Mathworks).

Referencing from a common, distant electrode has been shown to bias the interpretation of signals and to cause spurious correlations (Lalla et al., 2017; Shirhatti et al., 2016). In order to minimize this, subtractions of the signal in the PrL and HPC were performed between local pairs of electrodes. Based on the histological reconstruction, the electrode centered in each region of interest (left HPC, right HPC, and PrL) was re-referenced to its closest neighbor. All data analysis was then performed on the three resulting localized signals from the left HPC, right HPC, and PrL, respectively.

2.7 | Recording sessions

Rats were tested for 10 min at the beginning of a single recording session. They were consecutively stimulated at the RPO and PAG-freezing thresholds established before. The first 1-s RPO train was delivered, followed 30 s later by an 8-s PAG train (Figure 3b), and at the end of the recording period, the rat had received 10 stimulations of each type (Figure 3a).

2.8 | Data processing

Given that PAG stimulation periods are eight times longer than RPO stimulation, 1-s segments of EEG were extracted from each stimulation event in order to adequately compare the effects of the two stimulation types. One-second periods of data before the onset of each event were extracted from each epoch, and treated as a control "pre-stimulation period," and the difference between this and the 1-s periods after the onset "during stimulation" was used for assessing stimulation effects (Figure 3b).

After segmentation of the data, each 1-s epoch was individually assessed for power, instantaneous frequency, coherence, pairwise phase consistency (PPC), and partial directed coherence (PDC). All 10 trials of each type within the session were then averaged for each measure within the "hippocampal theta" range (5–10 Hz).

2.9 | Spectral analysis

The time–frequency analyses reported here were done with two 1-s windows with 500 ms overlap between them that contains a trailing or leading 250 ms after or before the start of stimulation, respectively. All spectral analyses were carried out using the multi-taper method, with three tapers and a numerical bandwidth product of 5 from the Chronux package (http://chronux.org/; Bokil et al., 2010; Mitra, 2007)

and with a cut-off frequency set to 30 Hz. Note that the primary (central) taper of the three constitutes a Hanning window (i.e., cosine wave) that captures maximum power in the central 500 ms and little power in the leading/trailing 250 ms on either side. The secondary and tertiary tapers extend the width of this capture to some extent. Averaging across the three provides important smoothing of the spectral density estimation and coherence estimation. Here, we defined "theta" as 5–10 Hz and *z*-scored power spectral density for this band was calculated relative to the rest of the frequency spectrum.

2.10 | Pairwise phase consistency analysis

Supplementary to coherence analysis, PPC was also applied. PPC calculates the distribution of the relative angular distances between two Hilbert-transformed signals and estimates the phase coupling from the two based on the outcome. Unlike spectral coherence or phase-lock value estimates, PPC has been demonstrated to be free of the biases that come from a small number of observations (Vinck et al., 2010)—that is, a tendency for phase-lock values to not only be overestimated as sample size decreases but for the overestimates to converge at lower *N* (their figs. 2 and 4). In numerical terms, the PPC is equivalent to the square of the phase-locking value or coherence (and so is directly related to proportion of variance accounted for).

2.11 | Partial directed coherence analysis

To assess the direction of theta modulation between HPC and PrL, we employed the PDC method developed by Baccala and Sameshima (2001) and as used previously in our laboratory with hippocampal recordings (Ruan et al., 2017; Young et al., 2017)—also see Young and Eggermont (2009) for discussion.

2.12 | Experimental design and statistical analysis

Each measure of interest had its variance distribution analyzed for normality. The correlations between the means and the variances of the samples were calculated, and the data were power transformed, when necessary, before repeated measures ANOVAs were performed. For the ANOVAs, orthogonal polynomial contrasts were extracted for dimensional factors using SPSS (IBM) with the structure of some organized to test specific a priori hypotheses (see below). The interactions between these contrasts were assessed, and the linear and quadratic components were derived, where the significant interactions between the different levels of treatments can be captured by significant polynomial trends. The use of these methods allows for 1 degree-of-freedom contrasts, which prevent the effects of sphericity; 1 degree-of-freedom contrasts are also statistical measures that are recommended in the *Publication Manual of the American Psychological Association* (Kirk, 2013).

For statistical testing, the data were arranged to test the hypothesis that our two electric stimulation treatments (PAG and RPO) produce different states before versus during stimulation and between themselves. Also, we anticipated that measurements in the two hippocampi would be similar to each other and different from PrL and organized the region data as a nominally linear sequence [L-HPC, PrL, R-HPC]. Therefore, the key contrasts assessed by SPSS were *PAG/RPO x Stim x Region[Linear]* and *PAG/RPO x Stim x Region[Quadratic]*—where "PAG/RPO" contrasts stimulation of PAG versus RPO, "Stim" contrasts the pre-stimulation epoch with post-stimulation, and for "region" a significant quadratic [+1 −2 +1] trend tests the hypothesis that PrL differs from the average of the two hippocampi, while the linear [−1 0 +1] trend tests for a left–right HPC difference, independent of PrL.

The data and results presented here come from raw values that have not been transformed except via *z*-scoring. This was decided once the numbers transformed to produce normal error distributions yielded *p*-values in the ANOVA that were not substantially different from the *p*-values from those for the raw numbers. Therefore, in order to keep the interpretation of the numbers easy, the untransformed numbers and their statistical test results are reported there.

2.13 | Histological methods

At the end of all testing, the rats were euthanized with pentobarbitone sodium (100 mg/kg, i.p.) transcardially perfused with normal saline solution, then 10% formaldehyde in saline, and placed in sucrose-10% formaldehyde solution for cryoprotection. After saturation (>5 days), the brains were blocked with a cryoprotecting gel (VWR Chemicals), sectioned at 90 μm on a freezing microtome, and stained with thionin. Mounted sections were digitized and electrode placements reconstructed according to the atlas of Paxinos and Watson (2007).

3 | RESULTS

3.1 | Histology

3.1.1 | Stimulation electrode placements

All rats included in experiment 1 and experiment 2 had stimulating electrodes located in the PAG and RPO. Their histologically reconstructed locations are detailed in Figure 1. Of the original 12 rats, 7 had PAG electrodes tips in the middle PAG (mPAG) as originally intended (black dots, ●, Figure 1a) and were analyzed for differences between PAG and RPO stimulation in experiment 1 (RPO sites for these rats are shown in Figure 1d). Five rats had PAG electrodes in the anterior PAG (aPAG) and were excluded from experiment 1. Experiment 2 directly compared the effects of aPAG (gray dots, ●, Figure 1a) and mPAG (●) stimulation. Figure 1b shows the variation in the parts of PAG with A-P location diagrammatically. Examples of electrode tracks are shown in Figure 1c (PAG) and Figure 1e (RPO).

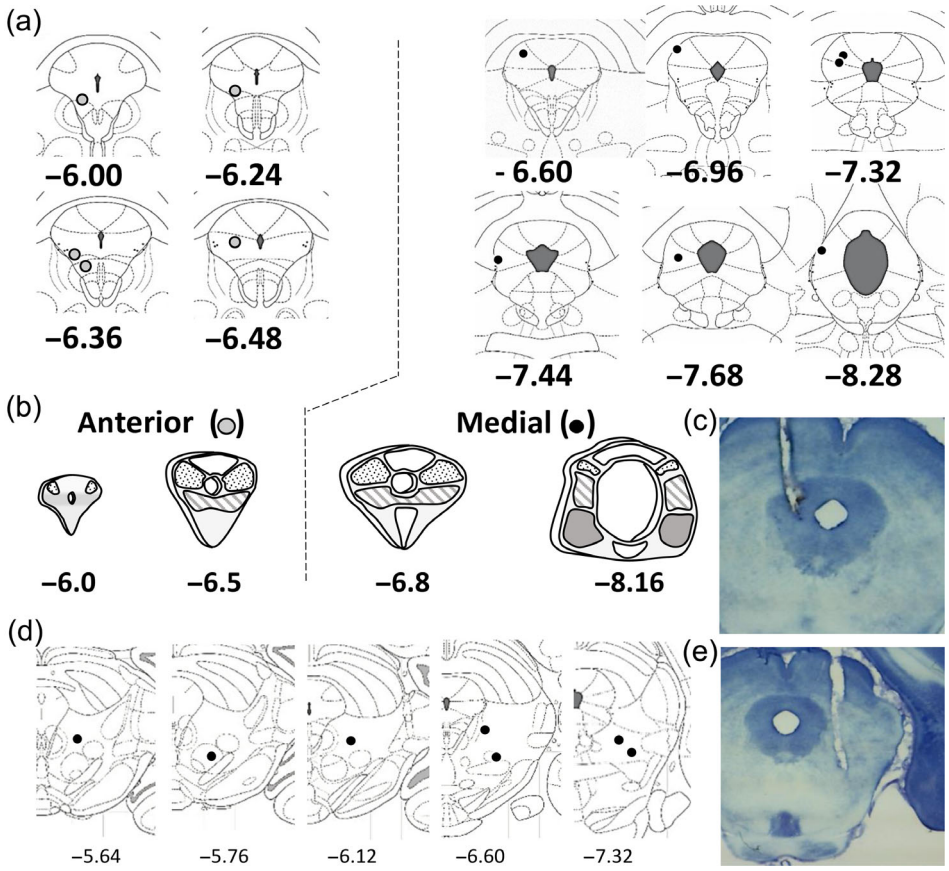

FIGURE 1 Histological placements of stimulating electrodes. Anterior PAG rats = gray dots; middle PAG rats = black dots. A–P coordinates from Bregma are indicated. (a) Black/gray dots indicate the locations of the anode of the two stimulating tips in each rat. (b) Diagrammatic representation of anterior-middle PAG boundary (*Source:* Adapted from Silva & McNaughton, 2019). (c) Representative example of histology from a PAG electrode. (d) Positions of RPO electrodes in experiment 1. (e) Representative example of histology from an RPO electrode. Line diagrams are taken from Paxinos and Watson (2007). PAG, periaqueductal gray

3.1.2 | Recording electrode placements

All rats had recording electrodes located in the left PrL and in the HPC, as well as stimulating electrodes located in the PAG and RPO. Histological locations for recording electrodes are detailed separately for rats with aPAG stimulating electrodes and mPAG stimulating electrodes (gray dots ● vs. black ●, respectively in Figure 2).

3.2 | Comparison of the effects of middle periaqueductal gray versus reticularis pontis oralis stimulation

3.2.1 | Behavioral and neural effects of stimulation: overview

For RPO stimulation, the maximum intensity that evoked theta rhythmicity with no motor manifestations averaged 57 μA across animals with ±4 μA (SEM) variations from 1 day to the next. This stimulation in the free-moving but stationary rats before PAG testing produced hippocampal theta of about 7–8 Hz.

For mPAG stimulation, the minimum current that elicited clear, repeatable, evoked freezing averaged 68 μA across animals with ±6.5 μA (SEM) variation across days. These effective mPAG currents caused evident freezing, with the arrest of ongoing motor activity and all four paws on the ground. Occasionally, these changes in posture would be accompanied by visible increases in breathing or chest movement patterns and sometimes micturition, defecation, or head scanning. A few seconds after the end of stimulation, the rats returned to normal behavior. With increased stimulation current (96 μA, ±9.6 μA as a group average), mPAG stimulation generated consistent escape behaviors, characterized by running forward and then in a circle because of the confined space while the stimulation train was on. This level of stimulation was not used during experimental testing.

As shown in Figure 3, mPAG stimulation provoked marked changes in HPC and left PrL field potentials that were bound to the stimulation period. With mPAG stimulation (panels c, d, and left-hand column of e) LFP amplitude is greatly diminished, during the stimulation period most clearly in the HPC. The effects of aPAG stimulation differ and a more detailed comparison between the two is provided in Section 3.3.1.

3.2.2 | Effects on local theta oscillations and non-directed connectivity

Figure 4 shows both raw spectral measures for pre-stimulation and during stimulation and the differences between real and pre-stimulation, that is, the effect of the stimulation. There were no major differences between mPAG and RPO during the pre-stimulation periods (i.e., immediately before stimulation) and so the text below focuses on the difference scores.

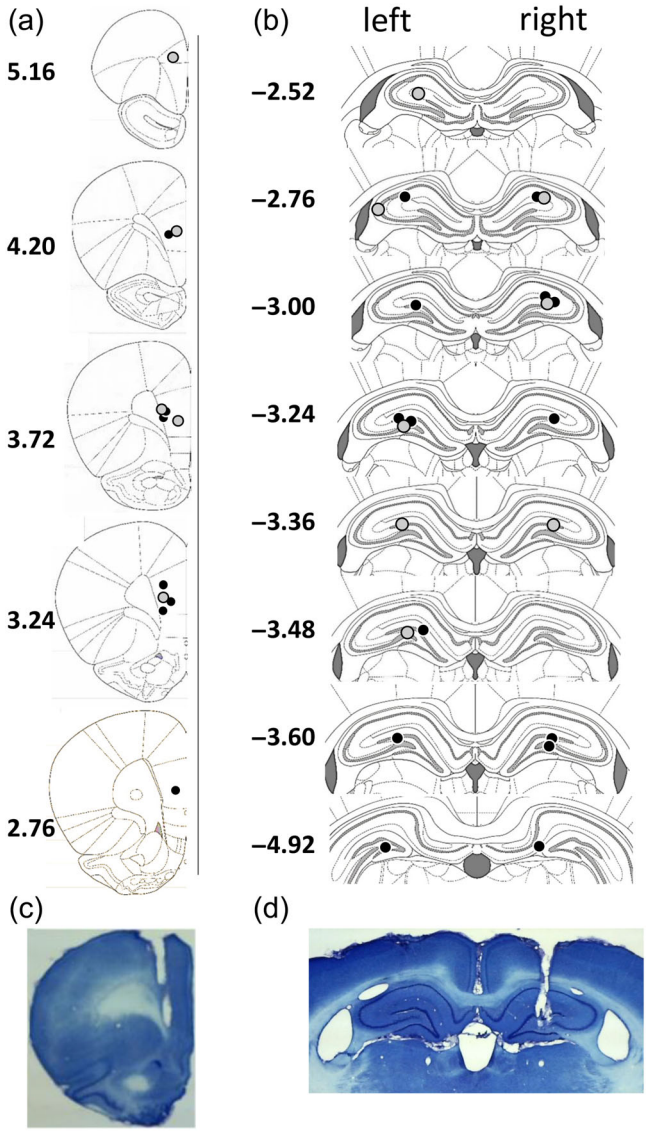

FIGURE 2 Histological placements of recording and electrodes. A-P coordinates from Bregma are indicated. Anterior PAG rats = gray dots; middle PAG rats = black dots. (a), (b) Dots indicate the center point between the pair of electrodes in each animal used for analysis. (a). PrL; (b). HPC. (c), (d) Representative photomicrographs with electrode tracks through, (c) the medial prefrontal cortex, and (d) dorsal hippocampus. Line diagrams are taken from Paxinos and Watson (2007). PAG, periaqueductal gray; PrL, prelimbic cortex

Theta power

Results for LFP power in the theta band are presented in Figure 4a. mPAG stimulation produced a large (~30%) decrease in LFP power (mPAG stimulation [linear], $F(1,6) = 52.61$, $p < .001$). RPO stimulation may have produced a slight increase in theta power (RPO stimulation [linear], $F(1,6) = 0.98$, $p = .36$) but even with L-HPC the apparent increase was not significant post hoc (RPO stimulation [linear], $F(1,6) = 1.61$, $p = .25$). There were no statistically significant higher order interactions. mPAG affected all three regions similarly. The apparent difference between PrL and the two HPC with RPO stimulation did not approach statistical significance (stimulation [linear] × region [quadratic], $F(1,6) = 1.78$, $p = .230$).

Theta frequency

Effects on frequency are presented in Figure 4b. RPO stimulation significantly reduced frequency (~0.4 Hz) across all recording sites (RPO stimulation [linear], $F(1,6) = 50.40$, $p < .001$). In contrast, mPAG stimulation dramatically reduced PrL theta frequency (to <6 Hz, i.e., near the bottom of the range HPC rhythmicity in free-moving rats), with the two HPC sites remaining largely unchanged (mPAG stimulation [linear] × region [quadratic], $F(1,6) = 298.60$, $p < .001$).

Theta coherence

Neither stimulation affected theta coherence significantly (Figure 4c). Importantly, neither the power nor frequency reductions in PrL were accompanied by any coherence reduction.

Theta pairwise phase consistency

The left and right HPC were generally more phase coherent with each other than with the PrL (region [quadratic], $F(1,5) = 7.61$, $p = .02$). No differences in theta PPC were seen between the two hippocampi and the PrL, that is, the left HPC shows similar theta phase consistency with the PrL to that of the right HPC (region [linear], $F(1,5) = 0.02$, $p = .87$). There were no significant differences between the pre-stimulation and stimulated periods with either mPAG or RPO stimulation.

3.2.3 | Effects on directed connectivity (partial directed coherence)

To assess the dynamics of causal influence between the HPCs and PrL through theta oscillations, PDC analysis was conducted. Figure 5a, c compare individual PDC measures for each direction (e.g., PrL → L-HPC vs. L-HPC → PrL) before and during stimulation. More focused comparisons are described below.

The pre-stimulation PDCs are shown as an average of RPO and PAG tests in Figure 5g (pre). Ignoring the effect of stimulation, the flow of information to the left PrL from the HPC (left and right) is larger than the flow from the left HPC to the right HPC (region [quadratic], $F(1,5) = 11.20$, $p = .02$). The right HPC tends to more strongly influence left PrL than does the left HPC, although the difference is marginal (region [linear], $F(1,5) = 6.48$, $p = .051$). Conversely, ignoring the effect of stimulation, the flow of information from the left PrL to the HPC (right or left) was not significantly different from that from the right to the left HPC (region [quadratic], $F(1,5) = 1.56$, $p = .266$). However, left PrL reliably influences the left HPC more than it influences the right HPC (region [linear], $F(1,5) = 23.69$, $p = .005$).

Difference scores (i.e., the effects of stimulation) are shown in Figure 5b,d,g [PAGΔ, RPOΔ, and netΔ]. There were no large changes with stimulation of either PAG or RPO. In the case of PAG stimulation

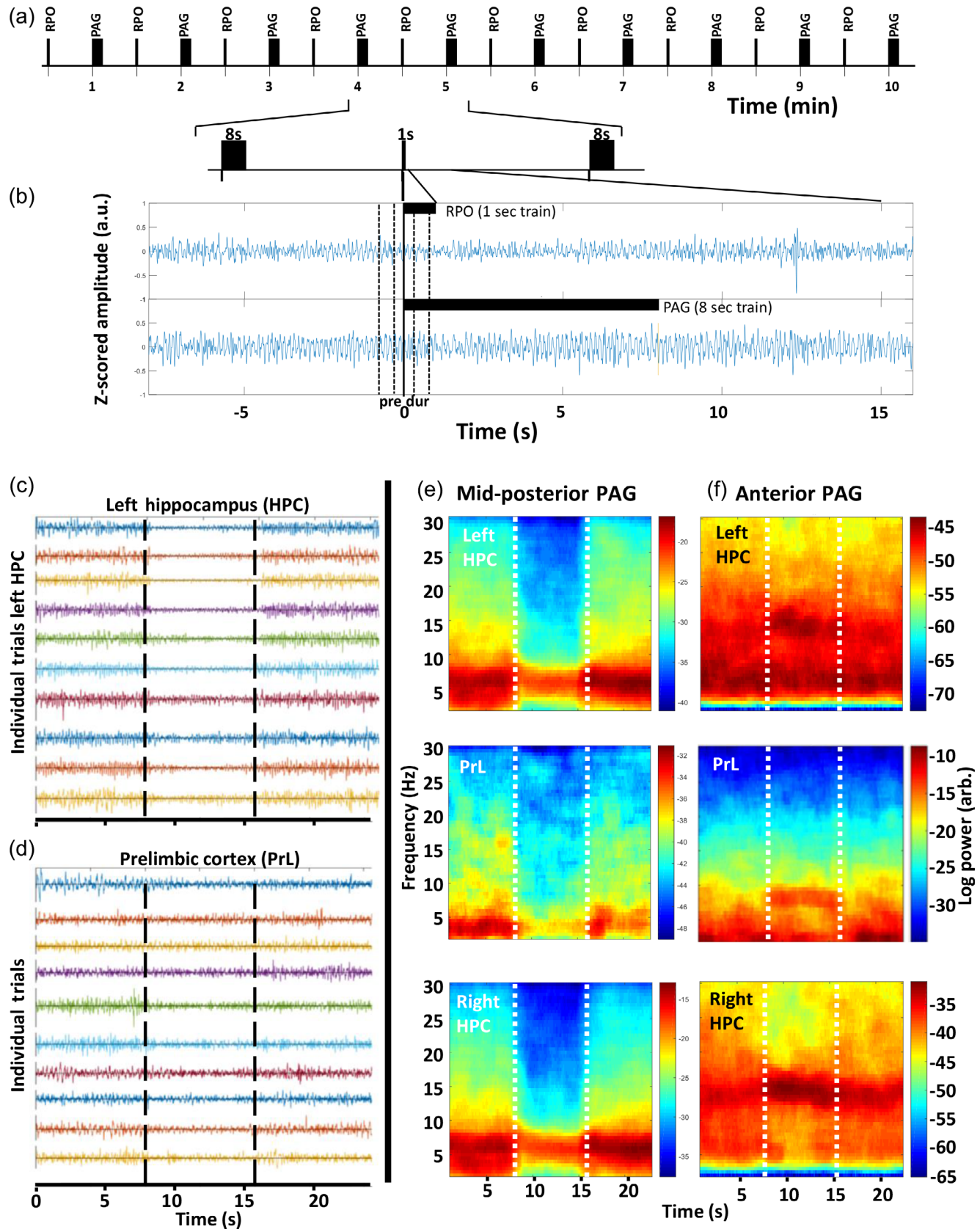

FIGURE 3 Examples of LFP activity under stimulation for representative mid-posterior PAG and anterior PAG rats. (a), (b) Representation of the organization and durations of stimulations and (dashed vertical lines) of the overlapping 1-s epochs before (pre) and during (dur) stimulation used for analysis. (c)–(e) Peri-stimulus periods of 8 s before, during, and after mPAG stimulation, which occur in the center period bounded by dashed lines. (c), (d) *z*-Scored LFP of 10 individual trials of mPAG stimulation. The *z*-scoring allows easy comparison of the wave form shapes but not their amplitudes. (c) Left HPC; (d) left PrL. (e) Averaged and log-transformed spectrograms of the same *z*-scored data as in (c) and (d) plus for right HPC. (f) Equivalent spectrograms from a rat with its stimulating electrode in the aPAG (see Section 3.3). PAG, periaqueductal gray

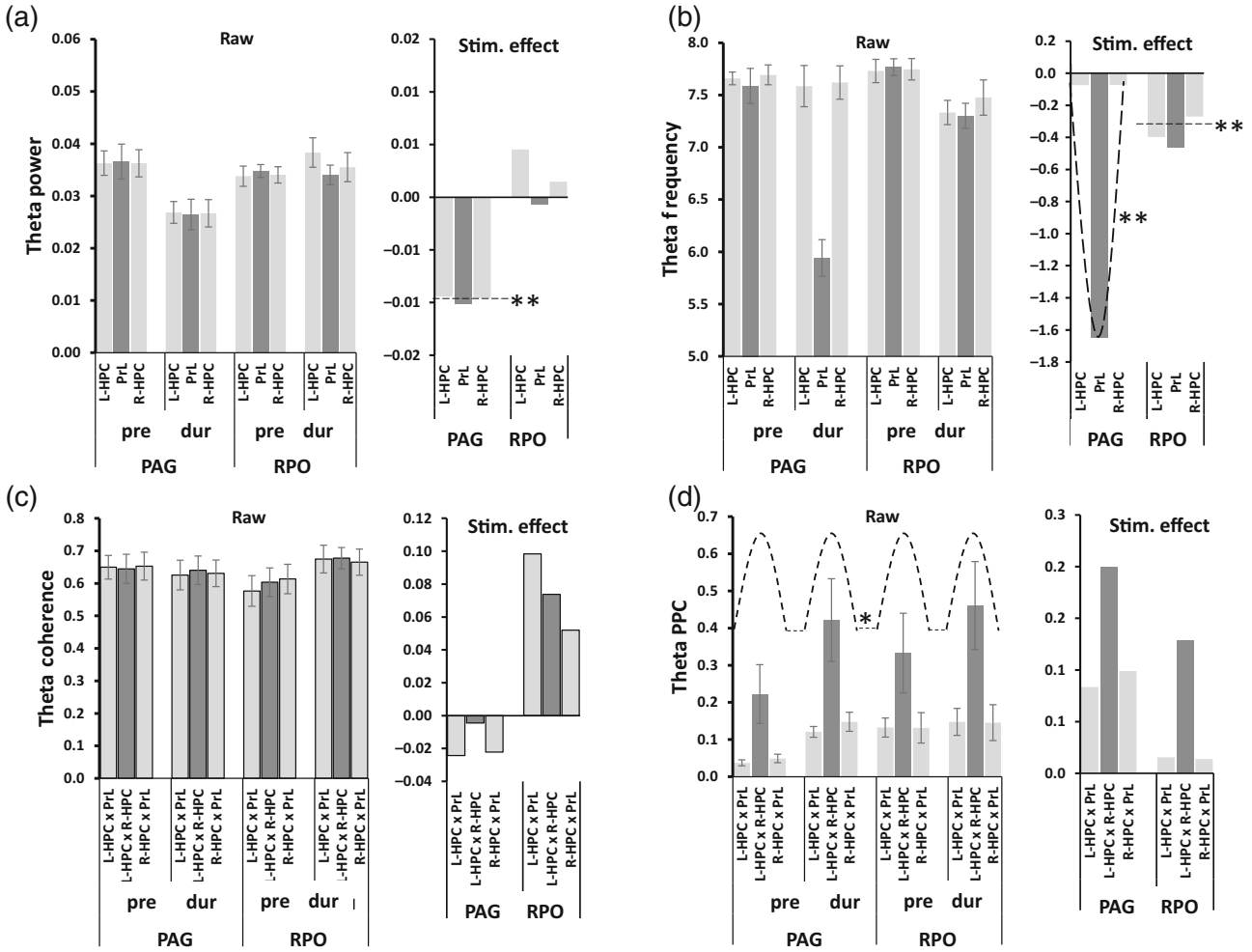

FIGURE 4 Theta parameters before (pre) or during (dur) stimulation of mPAG or RPO ($n = 7$). (a) Theta band power (arbitrary units). (b) Frequency (Hz). (c) Coherence. (d) PPC. The first of each pair of panels shows the raw data and the second shows the difference between during stimulation and pre-stimulation, that is, the effect of stimulation. The observed effects and differences are detailed in the text. Here and in the subsequent figures, statistically significant effects are illustrated with dashed lines and curves. Where a main effect applies to sets of data with no higher order interaction, this is illustrated with the same size curve for each included case, the curves are linked with straight lines and only a single p value is indicated (as in panel d). Separate post hoc effects (panels a, b) have unconnected curves each with their own p indicator. p values are indicated as $^{*}p < .05$ or $^{**}p < .01$. PAG, periaqueductal gray; PPC, pairwise phase consistency; RPO, reticularis pontis oralis

and HPC to PrL communication (Figure 5b,g [PAGΔ and netΔ]), neither the overall effect of stimulation nor the apparent variation across the areas was reliable (PAG post hoc: stimulation [linear], $F(1,5) = 3.28$, $p = .130$; stimulation [linear], $F(1,5) = 3.06$, $p = .141$). With RPO stimulation, however (Figure 5b,g [RPOΔ and netΔ]), L-HPC → PrL increased in contrast to R-HPC → PrL, which largely did not (RPO post hoc: stimulation × region [linear], $F(1,5) = 7.74$, $p = .039$). L-HPC → R-HPC did not increase and was significantly lower than the average of the two PrL cases (stimulation × region [quadratic], $F(1,5) = 15.52$, $p = .011$). With communication from PrL to HPC (Figure 5d,g), the flow of information from left PrL to both HPC and from R-HPC to L-HPC was not significantly affected with either type (PAG/RPO) of stimulation (stimulation × region [linear], $F(1,5) = 0.18$, $p = .686$; stimulation × region [quadratic], $F(1,5) = 0.01$, $p = .934$; PAG/RPO × stimulation × region [linear], $F(1,5) = 1.22$, $p = .32$; PAG/RPO × stimulation × region [quadratic], $F(1,5) = 0.08$, $p = .079$).

3.3 | Comparison of the effects of anterior periaqueductal gray with middle periaqueductal gray stimulation

In this section, we assess whether PAG stimulation of the five excluded rats with more anterior (aPAG) stimulating electrodes produced the same results as for the mPAG rats. All the results are reported as a direct comparison of aPAG with mPAG. Note that the

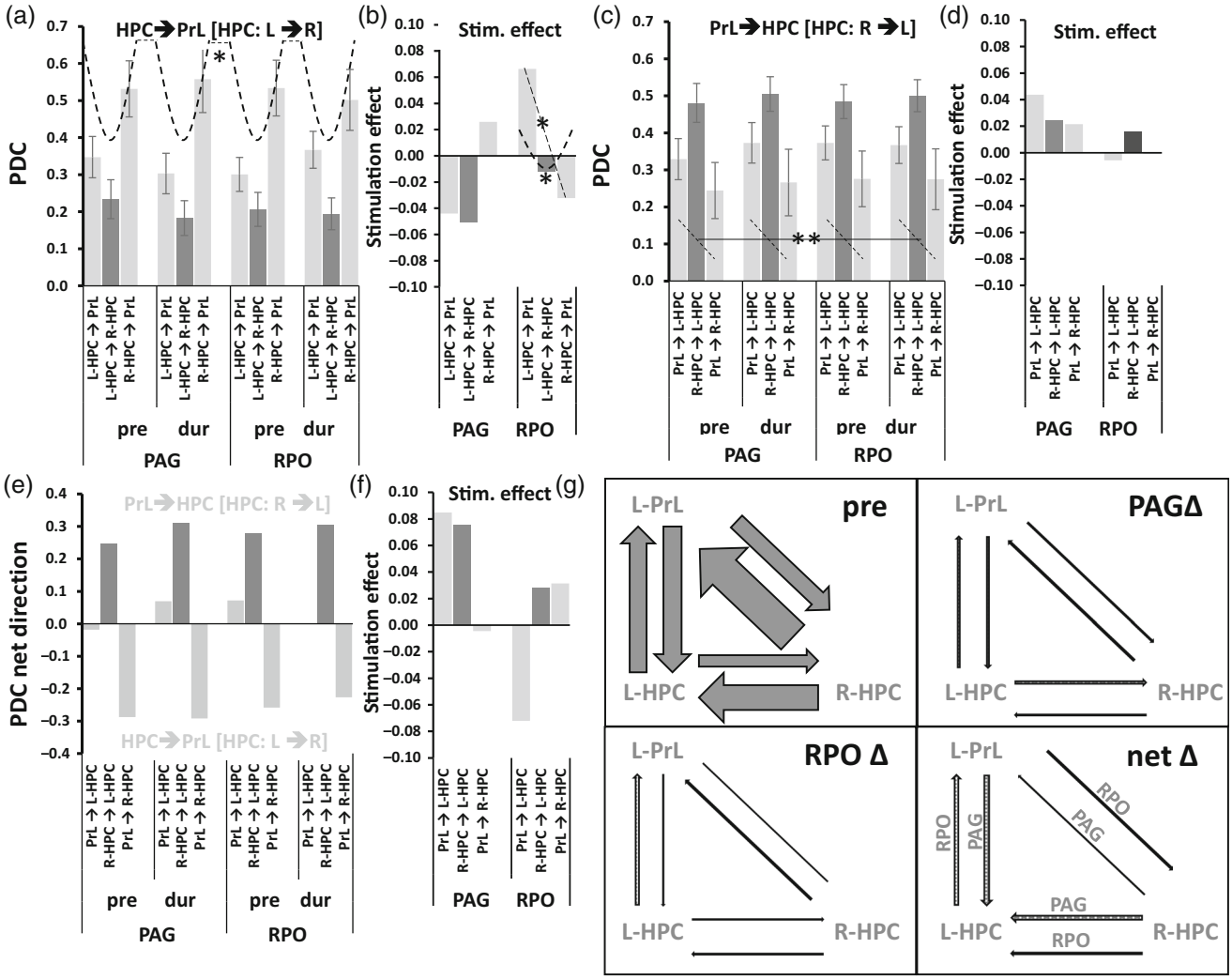

FIGURE 5 PDC before (pre) and during (dur) mPAG stimulation and RPO stimulation. (a), (b) For HPC → PrL and from left to right HPC. (c), (d) For PrL → HPC and from right to left HPC. (a), (c) Show pre and dur values. (b), (d) Show the pre-dur difference (i.e., the effect of stimulation; stim. effect). (e) The net PDC (c minus a) shown with net PrL → HPC as positive and net HPC → PrL as negative. (f) Stimulation effect (dur-pre) for the data in (e). (g) Diagrammatic representation of PDC with the width of the arrows equal to PDC value or difference: pre = average of PAG and RPO for pre; PAGΔ = PAG stimulation effect; RPOΔ = RPO stimulation effect; netΔ = net directional effect comparing RPO and PAG with the direction of the arrow determined by the sign of the net value. Statistical coding as in Figure 4. PAG, periaqueductal gray; PDC, partial directed coherence; PrL, prelimbic cortex; RPO, reticularis pontis oralis

raw mPAG data are the same as in Section 3.2 and are repeated for ease of graphical comparison and understanding of the difference scores.

3.3.1 | Behavioral and neural effects of stimulation: overview

The behaviors elicited by stimulation in the sites were partially distinct. As noted in Section 3.2.1, mPAG animals froze during stimulation, with occasional head scanning and faster breathing in some animals. aPAG stimulation also produced a form of freezing, but with a more consistent and intense occurrence of higher rates of breathing. aPAG stimulation also produced strong sniffing and occasional facial contractions during stimulation, which were completely absent in the mPAG rats.

With aPAG, the average minimum electric current that caused freezing was 428 μA, with a variation of ±6.9 μA (SEM) in different days of testing. This is considerably higher than with mPAG (68 μA, ±6.5 μA; t [10] = 3.88, p = .003). As noted above, higher levels of mPAG group stimulation generated escape behaviors, characterized by forward running in circles while the stimulation train was on. aPAG rats were more resistant to change of behaviors with higher currents; most consistently failing to show escape with stronger stimulation and usually remain frozen. Occasionally, higher currents in the aPAG group would cause backward locomotion, with an exaggerated arched back and lowered head. In some other animals, higher currents evoked strong, contralateral head-turning. These two behaviors are unique to aPAG animals, as no animals in the mPAG group displayed backing, hunching, or head-turning during stimulation.

Figure 3, which provides detailed traces and spectrograms for mPAG stimulation in panels c–e also has representative spectrograms for activity in the HPC and left PrL for an animal under aPAG stimulation (panel f). Comparison of e and f shows the difference between the spectrograms with the two types of stimulation.

In the mPAG rat, both left and right HPC had a dominating power band toward the bottom end of the 5–10 Hz range before stimulation. The low frequency is consistent with the rat being restricted in an operant chamber, and so confined to slower and smaller movements. During mPAG stimulation this band is still visible, but power is greatly reduced. Once stimulation is turned off, 5–10 Hz activity returns, with a rebound effect, in the HPC, of showing stronger power than during pre-stimulation. In contrast to HPC, for the left PrL, there is a clear power band below 5 Hz—although some modest oscillatory activity is also present at higher frequencies. During mPAG stimulation, as with HPC, PrL power is greatly reduced across all frequencies. Immediately after stimulation is turned off, theta power transiently recovers but, especially in the following seconds, is generally below the pre-stimulation level.

In the aPAG rat, pre-stimulation activity is somewhat different, with the rat shown having a much wider band of left HPC activity that is strong above 5 Hz and additional power increases at 15 Hz. aPAG stimulation produces a clear increase in 15 Hz HPC power with a modest reduction in the 5–10 Hz range in both hippocampi and no obvious rebound. With PrL recording, aPAG stimulation produces a modest increase in power in the region of 10 Hz, with a rebound below 5 Hz.

3.3.2 | Effects on local theta oscillations and non-directed connectivity

Figure 6 shows both raw theta measures for pre-stimulation and during stimulation and the difference between the two, that is, the effect of the stimulation. There were differences between aPAG and mPAG rats

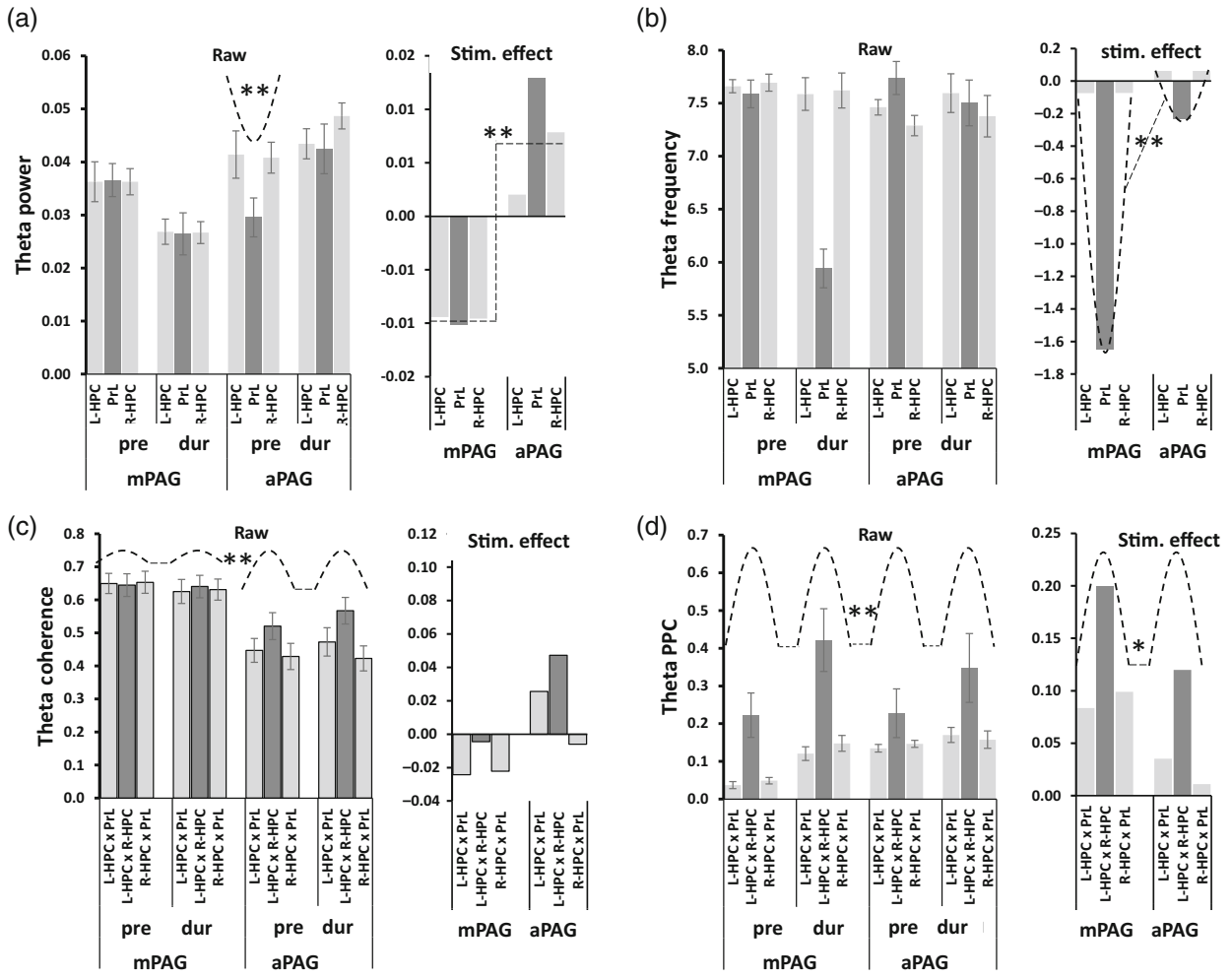

FIGURE 6 Theta parameters before (pre) or during (dur) stimulation of mPAG ($n = 7$) or aPAG ($N = 5$). (a) Theta band power (arbitrary units). (b) Frequency (Hz). (c) Coherence. (d) PPC. The first of each pair of panels shows the raw data and the second shows the dur-pre difference, that is, the effect of stimulation (stim. effect). The observed effects and differences are detailed in the text. Statistical coding as in Figure 4. PAG, periaqueductal gray; PPC, pairwise phase consistency

during the pre-stimulation periods (i.e., immediately before stimulation). For simplicity, and comparison with Section 3.2, the text below focuses on the difference scores and then notes the pre-stimulation differences.

Theta power (Figure 6a)

mPAG decreases but aPAG increases theta power across all regions relative to the prestimulus period (group × stimulation, $F[1,10] = 15.95$, $p = .003$) with no significant difference in the pattern across recording sites (group × stimulation × region [quadratic], $F[1,10] = 1.34$, $p = .274$). Averaged across the two stimulation periods there was a trend for lower power in PrL than HPC (group × region [quadratic], $F[1,10] = 5.17$, $p = .046$). Post hoc testing obtained a significant effect in the aPAG-pre-stimulation condition (region [quadratic], $F[1,4] = 22.78$, $p = .009$) but not the aPAG stimulated condition (region [quadratic], $F[1,4] = 0.31$, $p = .608$).

Theta frequency (Figure 6b)

There was a clear difference between the groups in terms of effects on PrL relative to HPC (group × stimulation × region [quadratic], $F(1,10) = 57.08$, $p < .001$). Unlike mPAG stimulation, aPAG stimulation does not greatly decrease PrL theta frequency (post hoc aPAG: stimulation × region [linear], $F(1,4) = 0.049$, $p = .83$; stimulation × region [quadratic], $F(1,4) = 5.70$, $p = .075$).

Theta coherence (Figure 6c)

There was higher coherence in the PrL region, relative to HPC regions in the aPAG but not the mPAG group overall (group × region

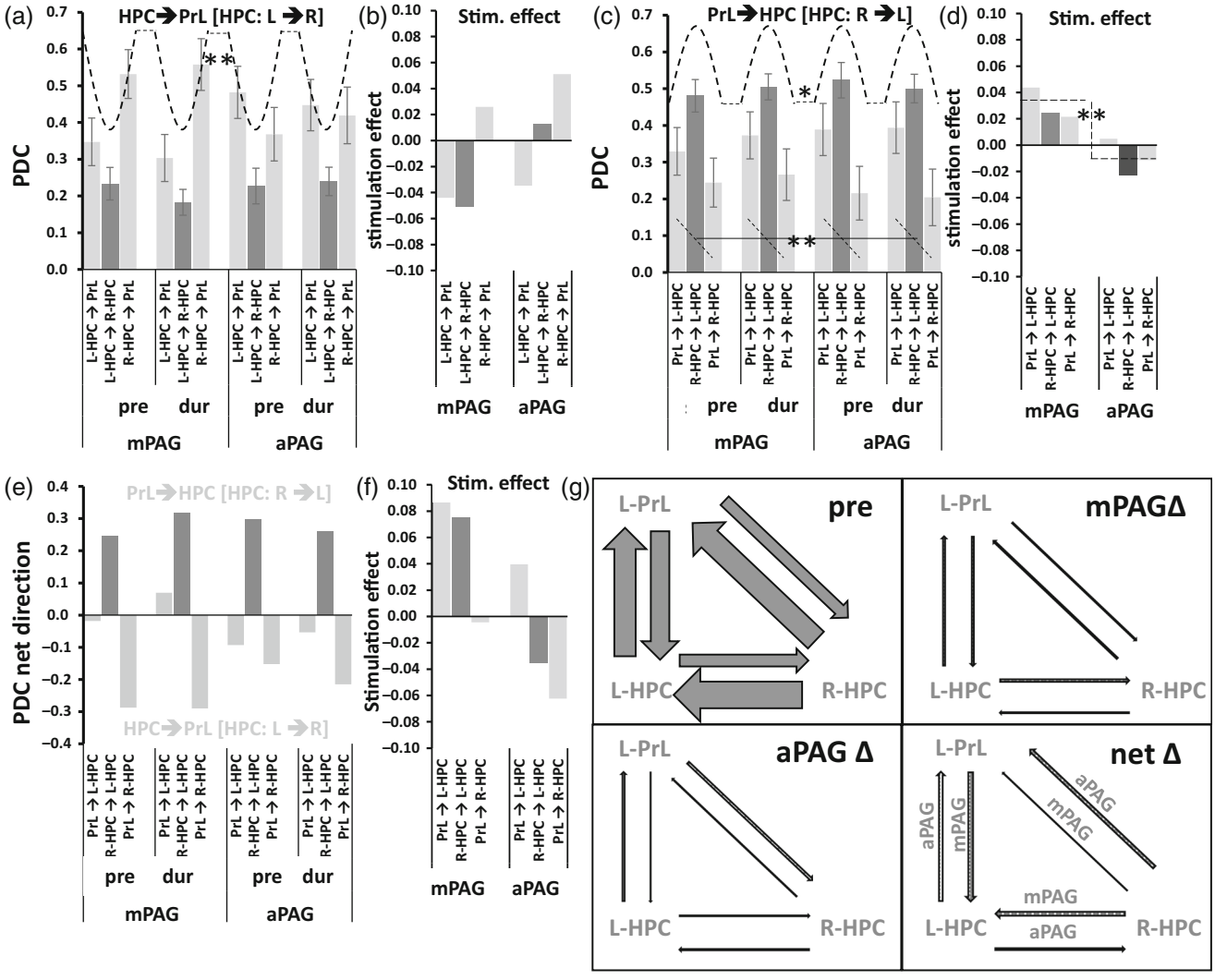

FIGURE 7 PDC before (pre) and during (dur) mPAG stimulation and aPAG stimulation. (a), (b) For HPC → PrL and from left to right HPC. (c), (d) For PrL → HPC and from right to left HPC. (a), (c) Show pre and dur values. (b), (d) Show the pre–dur difference (i.e., the effect of stimulation; stim. effect). (e) The net PDC (c minus a) shown with net PrL → HPC as positive and net HPC → PrL as negative. (f) Stimulation effect (dur–pre) for the data in (e). (g) Diagrammatic representation of PDC with the width of arrow equal to PDC value or difference: pre = average of mPAG and aPAG for pre; mPAGΔ = mPAG stimulation effect; aPAGΔ = aPAG stimulation effect; netΔ = net directional effect comparing aPAG and mPAG with the direction of arrows determined by the sign of the net value. Statistical coding as in Figure 4. PAG, periaqueductal gray; PDC, partial directed coherence; PrL, prelimbic cortex

[quadratic], $F(1,10) = 50.68$, $p < .001$), which was clearly present in the pre-stimulation condition (post hoc: group × region [quadratic], $F(1,10) = 11.91$, $p = .006$). There was no interaction of these group effects with stimulation (all $F(1,10) < 1.0$, $p > .3$).

Theta pairwise phase consistency (Figure 6d)

Stimulation generally increased PPC overall (stimulation, $F[1,9] = 47.95$, $p < .001$) but somewhat less so with aPAG than mPAG (group × stimulation, $F[1,9] = 7.40$, $p = .024$). PPC was highest overall between the HPC pair (pair [quadratic], $F[1,9] = 12.80$, $p = .006$) particularly with stimulation (stimulation × pair [quadratic], $F[1,9] = 8.53$, $p = .017$) and this was true for both aPAG and mPAG (group × pair [quadratic], $F(1,9) = 0.62$, $p = .450$; group × stimulation × pair [quadratic], $F(1,9) = 0.03$, $p = .877$).

3.3.3 | Effects on directed connectivity (partial directed coherence)

HPC to PrL PDC in the theta range (Figure 7) was greater than from L-HPC to R-HPC (region [quadratic], $F(1,9) = 24.96$, $p = .001$) and this did not vary with group, stimulation or their interaction (all $F(1,9) < 1.0$, $p > 0.4$). There may have been a tendency for left and right HPC to differ in their directed coherence to PrL both between groups (group × region [linear], $F(1,9) = 4.99$, $p = .052$) and in terms of the effects of stimulation (stimulation × region [linear], $F(1,9) = 4.55$, $p = .062$); but there was no substantial difference in the effects of stimulation between the groups (stimulation × group, $F(1,9) = 4.10$, $p = .074$; stimulation × region [linear] × group, $F(1,9) = 0.047$, $p = .83$; stimulation × region [quadratic] × group, $F(1,9) = 0.70$, $p = .42$).

PrL to HPC theta PDC was somewhat less than from R-HPC to L-HPC (region [quadratic], $F(1,9) = 5.24$, $p = .048$) and this did not vary with group, stimulation, or their interaction (all $F(1,9) < 0.6$, $p > .8$). PrL had higher directed coherence to L-HPC than R-HPC (region [linear], $F(1,9) = 11.14$, $p = .009$). mPAG and aPAG differed overall in the effects of stimulation (stimulation × group, $F(1,9) = 11.07$, $p = .009$); but there was no difference in the effects of stimulation between across regions (stimulation × region [linear], $F(1,9) = 1.19$, $p = .30$; stimulation × region [quadratic], $F(1,9) = 0.05$, $p = .92$; stimulation × region [linear] × group, $F(1,9) = 0.029$, $p = .87$; stimulation × region [quadratic] × group, $F(1,9) = 0.01$, $p = .93$).

4 | DISCUSSION

Stimulation of the mPAG that induced freezing without escape reduced the power of both HPC and PrL theta by ~30%. The reductions ceased as soon as stimulation was terminated, with a rebound in HPC theta power to a level above the pre-stimulation period. mPAG stimulation reduced PrL theta frequency to below 6 Hz (close to the HPC minimum for free moving animals) but did not affect HPC theta frequency.

In contrast to mPAG, RPO stimulation tended to produce a slight *increase* in HPC (but not PrL) power; and produced a small but significant reduction in frequency (from ~7.7 to ~7.3 Hz) in both HPC and PrL. While small, this drop in frequency contrasts with the usual increase (Green & Arduini, 1954; McNaughton & Sedgwick, 1978; Vertes, 1981). In free-moving but stationary rats, 100 Hz 0.1 ms stimulation produces HPC theta of 7–8 Hz with 50 μA pulses (McNaughton & Sedgwick, 1978, fig. 1); our pre-test adjustments of RPO stimulation also used ~50 μA, and generated 7–8 Hz HPC theta against a background of no theta. However, during our comparison of mPAG and RPO, HPC theta was already at 7.5 Hz before the onset of stimulation. We did not explicitly monitor movement but, even without movement, our repeated activation of the mPAG (see also discussion of aPAG) at the threshold of freezing could have conditioned an emotional state that resulted in high basal theta activity in the hippocampus (Mikulovic et al., 2018; Sainsbury, Heynen, & Montoya, 1987). The results suggest that the stimulation of RPO output axons overrides the effect of the normal inputs to RPO. That is, the stimulation would orthodromically activate structures such as the supramammillary area to generate theta frequency (Kirk & McNaughton, 1993) but antidromically activate RPO cell bodies and so block, via collision, the effects of ongoing normal input to RPO.

Coherence, PPC, and PDC measures showed no significant change with either mPAG or RPO stimulation despite clear connectivity both before and during stimulations. PPC and PDC (but not simple coherence) indicated lesser connectivity for PrL → HPC than other connections. This is consistent with the finding that mPAG stimulation reduces PrL but not HPC theta frequency.

Our aPAG stimulation was similar to mPAG stimulation in generating freezing without escape. As with mPAG, aPAG stimulation did not produce any clear changes in coherence, PPC, or phase-directed coherence. However, the aPAG group results differed from mPAG in other respects as detailed below and in ways that are consistent with an antagonistic relationship between panic (and perhaps fear in general) with anxiety (Deakin & Graeff, 1991).

First, it is likely that aPAG stimulation produced a different form of freezing to mPAG, with more high-rate breathing, strong sniffing, and occasional facial contractions during stimulation. Critically, high levels of aPAG stimulation continued to elicit freezing without generating escape.

Second, aPAG had different pre-stimulation recordings to mPAG. aPAG rats had higher power at higher frequencies (10 Hz and above) compared to mPAG rats (Figure 3). Also, in the 5–10 Hz range analyzed, the aPAG group had higher baseline HPC power (but somewhat less PrL power) and a tendency to a lower HPC frequency. Since aPAG and mPAG rats were only separated after histology, it seems likely (as argued above) that the presence of substantial theta in the absence of stimulation was the result of conditioning (or some after effect of PAG stimulation) with the state generated by aPAG stimulation being different from mPAG and so resulting in different after-effects. Note that RPO stimulation does not generate such post-stimulus activation; and, with standard RPO testing, there is a tendency for the rats to become somnolent with long periods of testing and so produce no background theta.

Third, aPAG stimulation (like RPO stimulation) caused increases in power while mPAG caused decreases. The increases in power with aPAG stimulation were greatest for PrL, less for R-HPC, and negligible for L-HPC. The PrL change reflected a shift to equality with HPC from its before-stimulation lower power.

Fourth, aPAG stimulation (like RPO stimulation) did not produce the clear reduction in prefrontal frequency seen with mPAG. However, as with power, there appears to be a trend to equalization of PrL with HPC compared to before stimulation.

In interpreting these results we should keep in mind the nature of RPO-elicited theta. The reduction in this elicitation is a reliable predictor of clinical anxiolytic action (McNaughton et al., 2007); but RPO-elicited theta is not accompanied by any behavioral changes or signs of arousal under normal drug-testing conditions. HPC theta also occurs more generally in response to important (either positive or negative) events. As examples, HPC theta is generated by: hunger and food (Ford et al., 1970; Munn et al., 2015; Routtenberg, 1968), predators (Mikulovic et al., 2018; Sainsbury, Heynen, & Montoya, 1987), operant learning (Feder & Ranck, 1973; Lopes da Silva & Kamp, 1969), novel stimuli (Kemp & Kaada, 1975), and known but important stimuli (Pena et al., 2017). Conversely, irrelevant stimuli or habituated stimuli (Kemp & Kaada, 1975; Sainsbury, Harris, & Rowland, 1987), well-learned behaviors, automatic behaviors (Feder & Ranck, 1973), and consummatory acts (Routtenberg, 1968) do not generate HPC theta. Theta therefore appears to control a process that is important for sustaining clinical anxiety but, at least when elicited by RPO stimulation, does not represent an anxious state as such.

aPAG stimulation in the current experiments had much the same electrophysiological effects as RPO stimulation but, in addition, produced a form of freezing coupled with a range of other reactions consistent with an elicited state of anxiety. The data also suggest that this elicited anxiety became conditioned to the apparatus to at least some extent: producing theta that would not otherwise have been observed (e.g., as in the RPO-alone stimulation we used in preliminary assessment). mPAG stimulation, by contrast, seemed to produce a somewhat different form of freezing and, at higher intensities, undirected escape reactions—consistent with the conventional interpretation that it elicits panic/fear (Deakin & Graeff, 1991; Evans et al., 2018). Contextual fear conditioning is normally seen as generating anxiety (i.e., anxiolytic-sensitive reactions) rather than fear (León et al., 2017; Luyten et al., 2011) and so it is not surprising that, like aPAG, mPAG stimulation appears to condition a state with high background theta. However, the mPAG unstimulated theta has less variation between the recoding sites (with PrL having lower power and higher frequency in the mPAG case than aPAG). These differences could be because the unconditioned states are qualitatively different or simply because they produce different amounts of contextual conditioning. Critically, whatever the specific causal chains involved, the data are consistent with anxiety (or anxiety processing states) being linked to theta and suppression of such anxiety-related processes by panic/fear in general and mPAG stimulation in particular, including reports from humans (see Carrive & Morgan, 2012). Our data are also consistent with theories of the parallel hierarchical neural organization of fear and anxiety systems extending from the prefrontal cortex down to the PAG (Silva & McNaughton, 2019).

ACKNOWLEDGMENTS

Carlos Silva was supported by a doctoral scholarship from the Ministério da Educação, Coordenação de Aperfeiçoamento de Pessoal de Nível Superior—CAPES, Brazil. Open access publishing facilitated by University of Otago, as part of the Wiley - University of Otago agreement via the Council of Australian University Librarians.

CONFLICT OF INTEREST

The authors declare no competing financial interests.

DATA AVAILABILITY STATEMENT

The data that support the findings of this study are available from the corresponding author upon reasonable request. The Spike2 files containing the original data are available via Mendeley Data (Silva et al., 2022).

ORCID

Carlos Silva https://orcid.org/0000-0003-3488-5241
Calvin K. Young https://orcid.org/0000-0002-6130-8370
Neil McNaughton https://orcid.org/0000-0003-4348-8221

REFERENCES

Adhikari, A., Topiwala, M. A., & Gordon, J. A. (2010). Synchronized activity between the ventral hippocampus and the medial prefrontal cortex during anxiety. *Neuron*, *65*(2), 257–269.

Baccala, L. A., & Sameshima, K. (2001). Partial directed coherence: A new concept in neural structure determination. *Biological Cybernetics*, *84*(6), 463–474.

Bannerman, D. M., Rawlins, J. N. P., McHugh, S. B., Deacon, R. M. J., Yee, B. K., Bast, T., Zhang, W. N., Pothuizen, H. H. J., & Feldon, J. (2004). Regional dissociation within the hippocampus—Memory and anxiety. *Neuroscience & Biobehavioral Reviews*, *28*, 273–283.

Banstola, A., Silva, C., Ulrich, K., Ruan, M., Robertson, L., & McNaughton, N. (2021). Construction of simple, customised, brain-spanning multi-channel linear microelectrode arrays. *Journal of Neuroscience Methods*, *348*, 109011.

Blanchard, D. C., & Blanchard, R. J. (1990a). Effects of ethanol, benzodiazepines and serotonin compounds on ethopharmacological models of anxiety. In N. McNaughton & G. Andrews (Eds.), *Anxiety* (pp. 188–200). University of Otago Press.

Blanchard, R. J., & Blanchard, D. C. (1990b). Anti-predator defense as models of animal fear and anxiety. In P. F. Brain, S. Parmigiani, R. J. Blanchard, & D. Mainardi (Eds.), *Fear and defence* (pp. 89–108). Chur, Switzerland.

Bokil, H., Andrews, P., Kulkarni, J. E., Mehta, S., & Mitra, P. P. (2010). Chronux: A platform for analyzing neural signals. *Journal of Neuroscience Methods*, *192*(1), 146–151.

Carrive, P., & Morgan, M. M. (2012). Periaqueductal gray. In J. K. Mai & G. Paxinos (Eds.), *The human nervous system* (3rd ed., pp. 367–400). Elsevier.

Cohen, A. S., Barlow, D. H., & Blanchard, E. B. (1985). Psychophysiology of relaxation-associated panic attacks. *Journal of Abnormal Psychology*, *94*(1), 96–101.

Conti, L. H., Maciver, C. R., Ferkany, J. W., & Abreu, M. E. (1990). Foot-shock-induced freezing behavior in rats as a model for assessing anxiolytics. *Psychopharmacology*, *102*(4), 492–497.

Davidson, T., Kanoski, S. E., Walls, E. K., & Jarrard, L. E. (2005). Memory inhibition and energy regulation. *Physiology & Behavior*, *86*(5), 731–746.

Davidson, T. L., Chan, K., Jarrard, L. E., Kanoski, S. E., Clegg, D. J., & Benoit, S. C. (2009). Contributions of the hippocampus and medial prefrontal cortex to energy and body weight regulation. *Hippocampus*, *19*(3), 235–252.

De Molina, A. F., & Hunsperger, R. W. (1962). Organization of the subcortical system governing defense and flight reactions in the cat. *Journal of Physiology*, *160*, 200–213.

Deakin, J. F. W., & Graeff, F. G. (1991). 5-HT and mechanisms of defence. *Journal of Psychopharmacology*, *5*(4), 305–315.

Evans, D. A., Stempel, A. V., Vale, R., Ruehle, S., Lefler, Y., & Branco, T. (2018). A synaptic threshold mechanism for computing escape decisions. *Nature*, *558*(7711), 590–594.

Feder, R., & Ranck, J. B., Jr. (1973). Studies on single neurons in dorsal hippocampal formation and septum in unrestrained rats. II. Hippocampal slow waves and theta cell firing during bar pressing and other behaviors. *Experimental Neurology*, *41*(2), 532–555.

Ford, J. G., Bremner, F. J., & Richie, W. R. (1970). The effect of hours of food deprivation on hippocampal theta rhythm. *Neuropsychologia*, *8*(1), 65–73.

Gordon, J. A. (2011). Oscillations and hippocampal–prefrontal synchrony. *Current Opinion in Neurobiology*, *21*(3), 486–491.

Gray, J. A., & McNaughton, N. (2000). *The neuropsychology of anxiety: An enquiry into the functions of the septo-hippocampal system* (2nd ed.). Oxford University Press.

Green, J. D., & Arduini, A. A. (1954). Hippocampal electrical activity in arousal. *Journal of Neurophysiology*, *17*(6), 533–557.

Jenck, F., Moreau, J. L., & Martin, J. R. (1995). Dorsal periaqueductal Gray-induced aversion as a simulation of panic anxiety—Elements of face and predictive-validity. *Psychiatry Research*, *57*(2), 181–191.

Kemp, I. R., & Kaada, B. R. (1975). The relation of hippocampal theta activity to arousal, attentive behaviour and somato-motor movements in unrestrained cats. *Brain Research*, *95*(2–3), 323–342.

Kirk, I. J., & McNaughton, N. (1993). Mapping the differential effects of procaine on frequency and amplitude of reticularly elicited hippocampal rhythmical slow activity. *Hippocampus*, *3*, 517–526.

Kirk, R. (2013). *Experimental design: Procedures for the behavioral sciences*. Sage Publications Inc.

Klein, D. F. (1993). False suffocation alarms, spontaneous panics, and related conditions—An integrative hypothesis. *Archives of General Psychiatry*, *50*(4), 306–317.

Lalla, L., Rueda Orozco, P. E., Jurado-Parras, M. T., Brovelli, A., & Robbe, D. (2017). Local or not local: Investigating the nature of striatal theta oscillations in behaving rats. *eNeuro*, *4*(5), ENEURO.0128-17.2017.

Lathe, R. (2001). Hormones and the hippocampus. *Journal of Endocrinology*, *169*(2), 205–231.

Lathe, R. (2004). The individuality of mice. *Genes, Brain and Behavior*, *3*, 317–327.

LeDoux, J. E. (2012). Rethinking the emotional Brain. *Neuron*, *73*(4), 653–676.

LeDoux, J. E. (2015). *Anxious: The modern mind in the age of anxiety*. Oneworld Publications.

LeDoux, J. E. (2021). As soon as there was life, there was danger: The deep history of survival behaviours and the shallower history of consciousness. *Philosophical Transactions of the Royal Society B: Biological Sciences*, *377*(1844), 20210292.

León, L. A., Castro-Gomes, V., Zárate-Guerrero, S., Corredor, K., Mello Cruz, A. P., Brandão, M. L., Cardenas, F. P., & Landeira-Fernandez, J. (2017). Behavioral effects of systemic, infralimbic and prelimbic injections of a serotonin 5-HT2A antagonist in carioca high- and low-conditioned freezing rats. *Frontiers in Behavioral Neuroscience*, *11*(117), A117.

da Lopes, Silva, F. H., & Kamp, A. (1969). Hippocampal theta frequency shifts and operant behaviour. *Electroencephalography and Clinical Neurophysiology*, *26*(2), 133–143.

Luyten, L., Vansteenwegen, D., van Kuyck, K., Gabriëls, L., & Nuttin, B. (2011). Contextual conditioning in rats as an animal model for generalized anxiety disorder. *Cognitive, Affective, & Behavioral Neuroscience*, *11*(2), 228–244.

Magierek, V., Ramos, P. L., da Silveira-Filho, N. G., Nogueira, R. L., & Landeira-Fernandez, J. (2003). Context fear conditioning inhibits panic-like behavior elicited by electrical stimulation of dorsal periaqueductal gray. *Neuroreport*, *14*, 1641–1644.

McIntyre, D. C., & Molino, A. (1972). Amygdala lesions and CER learning: long term effect of kindling. *Physiology & behavior*, *8*(6), 1055–1058.

McNaughton, N., & Gray, J. A. (2000). Anxiolytic action on the behavioural inhibition system implies multiple types of arousal contribute to anxiety. *Journal of Affective Disorders*, *61*, 161–196.

McNaughton, N., Kocsis, B., & Hajós, M. (2007). Elicited hippocampal theta rhythm: A screen for anxiolytic and procognitive drugs through changes in hippocampal function? *Behavioural Pharmacology*, *18*(5–6), 329–346.

McNaughton, N., & Morris, R. G. M. (1987). Chlordiazepoxide, an anxiolytic benzodiazepine, impairs place navigation in rats. *Behavioural Brain Research*, *24*, 39–46.

McNaughton, N., & Morris, R. G. M. (1992). Buspirone produces a dose-related impairment in spatial navigation. *Pharmacology, Biochemistry and Behavior*, *43*, 167–171.

McNaughton, N., Ruan, M., & Woodnorth, M. A. (2006). Restoring theta-like rhythmicity in rats restores initial learning in the Morris water maze. *Hippocampus*, *16*, 1102–1110.

McNaughton, N., & Sedgwick, E. M. (1978). Reticular stimulation and hippocampal theta rhythm in rats: Effects of drugs. *Neuroscience*, *3*, 629–632.

McNaughton, N., & Vann, S. D. (2022). Construction of complex memories via parallel distributed cortical-subcortical iterative integration. *Trends in neurosciences*, *45*(7), 550–562.

Mellman, T. A., & Uhde, T. W. (1989). Electroencephalographic sleep in panic disorder. A focus on sleep-related panic attacks. *Archives of General Psychiatry*, *46*(2), 178–184.

Mikulovic, S., Restrepo, C. E., Siwani, S., Bauer, P., Pupe, S., Tort, A. B. L., Kullander, K., & Leao, R. N. (2018). Ventral hippocampal OLM cells control type 2 theta oscillations and response to predator odor. *Nature Communications*, *9*(1), A3638.

Mitra, P. (2007). *Observed brain dynamics*. Oxford University Press.

Mobbs, D., & LeDoux, J. E. (2018). Editorial overview: Survival behaviors and circuits. *Current Opinion in Behavioral Sciences*, *24*, 168–171.

Munn, R. G., Tyree, S. M., McNaughton, N., & Bilkey, D. K. (2015). The frequency of hippocampal theta rhythm is modulated on a circadian period and is entrained by food availability. *Frontiers in Behavioral Neuroscience*, *9*, 61.

Padilla-Coreano, N., Canetta, S., Mikofsky, R. M., Alway, E., Passecker, J., Myroshnychenko, M. V., Garcia-Garcia, A. L., Warren, R., Teboul, E., Blackman, D. R., Morton, M. P., Hupalo, S., Tye, K. M., Kellendonk, C., Kupferschmidt, D. A., & Gordon, J. A. (2019). Hippocampal-prefrontal theta transmission regulates avoidance behavior. *Neuron*, *104*(3), 601–610.e4.

Papez, J. W. (1937). A proposed mechanism of emotion. *Archives of Neurological Psychiatry*, *38*, 725–743.

Paxinos, G., & Watson, C. (2007). *The rat brain in stereotaxic coordinates* (6th ed.). Academic Press.

Pena, R. R., Medeiros, D. C., Guarnieri, L. O., Guerra, J. B., Carvalho, V. R., Mendes, E., Pereira, G. S., & Moraes, M. F. D. (2017). Home-cage odors spatial cues elicit theta phase/gamma amplitude coupling between olfactory bulb and dorsal hippocampus. *Neuroscience*, *363*, 97–106.

Perusini, J. N., & Fanselow, M. S. (2015). Neurobehavioral perspectives on the distinction between fear and anxiety. *Learning & Memory*, *22*(9), 417–425.

Rhudy, J. L., & Meagher, M. W. (2000). Fear and anxiety: divergent effects on human pain thresholds. *Pain*, *84*(1), 65–75.

Routtenberg, A. (1968). Hippocampal correlates of consummatory and observed behavior. *Physiology & Behavior*, *3*(4), 533–535.

Ruan, M., Young, C. K., & McNaughton, N. (2017). Bi-directional theta modulation between the Septo-hippocampal system and the mammillary area in free-moving rats. *Frontiers in Neural Circuits*, *11*, 62.

Sainsbury, R. S., Harris, J. L., & Rowland, G. L. (1987). Sensitization and hippocampal type 2 theta in the rat. *Physiology & Behavior*, *41*(5), 489–493.

Sainsbury, R. S., Heynen, A., & Montoya, C. P. (1987). Behavioral correlates of hippocampal type 2 theta in the rat. *Physiology & Behavior*, *39*(4), 513–519.

Shirhatti, V., Borthakur, A., & Ray, S. (2016). Effect of reference scheme on power and phase of the local field potential. *Neural Computation*, *28*(5), 882–913.

Silva, C., & McNaughton, N. (2019). Are periaqueductal gray and dorsal raphe the foundation of appetitive and aversive control? A comprehensive review. *Progress in Neurobiology*, *177*, 33–72.

Silva, C., Young, C. K., & McNaughton, N. (2022). PAG-EEG_2022-04-17. Mendeley data V1. https://doi.org/10.17632/dwr96htx3j.1

Sudre, E. C., de Barros, M. R., Sudre, G. N., & Schenberg, L. C. (1993). Thresholds of electrically induced defence reaction of the rat: Short- and long-term adaptation mechanisms. *Behavioural Brain Research*, *58*(1–2), 141–154.

Tovote, P., Esposito, M. S., Botta, P., Chaudun, F., Fadok, J. P., Markovic, M., Wolff, S. B., Ramakrishnan, C., Fenno, L., Deisseroth, K., Herry, C., Arber, S., & Lüthi, A. (2016). Midbrain circuits for defensive behaviour. *Nature*, *534*(7606), 206–212.

Tracy, A. L., Jarrard, L. E., & Davidson, T. L. (2001). The hippocampus and motivation revisited: Appetite and activity. *Behavioural Brain Research*, *127*(2001), 13–23.

Vann, S. D., & Nelson, A. J. (2015). The mammillary bodies and memory: More than a hippocampal relay. *Progress in Brain Research*, *219*, 163–185.

Vertes, R. P. (1981). An analysis of ascending brain stem systems involved in hippocampal synchronization and desynchronization. *Journal of Neurophysiology*, *46*(5), 1140–1159.

Vinck, M., van Wingerden, M., Womelsdorf, T., Fries, P., & Pennartz, C. M. (2010). The pairwise phase consistency: A bias-free measure of rhythmic neuronal synchronization. *NeuroImage*, *51*(1), 112–122.

Young, C. K., & Eggermont, J. J. (2009). Coupling of mesoscopic brain oscillations: Recent advances in analytical and theoretical perspectives. *Progress in Neurobiology*, *89*(1), 61–78.

Young, C. K., & McNaughton, N. (2009). Coupling of theta oscillations between anterior and posterior midline cortex and with the hippocampus in freely behaving rats. *Cerebral Cortex*, *19*(1), 24–40.

Young, C. K., Ruan, M., & McNaughton, N. (2017). A critical assessment of directed connectivity estimates with artificially imposed causality in the supramammillary-septo-hippocampal circuit. *Frontiers in Systems Neuroscience*, *11*, 72.

How to cite this article: Silva, C., Young, C. K., & McNaughton, N. (2022). Prefrontal and hippocampal theta rhythm show anxiolytic-like changes during periaqueductal-elicited "panic" in rats. *Hippocampus*, *32*(9), 679–694. https://doi.org/10.1002/hipo.23459